Characteristics of Air Jets Discharging Normally into a Swirling Crossflow

Saad A. Ahmed* and Ronald M. C. So†
Arizona State University, Tempe, Arizona

Jets discharging normally into a swirling crossflow are investigated experimentally. Total jet to total swirling flow axial momentum ratios of 0.43 and 0.96 are examined. A vane swirler with an overall swirl number of 2.25 is used to generate the crossflow in a 125-mm i.d. tube. The jet nozzle with an exit diameter of 8.73 mm is mounted at one tube diameter downstream of the swirler. A one-color, one-component laser Doppler anemometer, operating in the forward scatter mode, is used to measure the flowfield downstream of the jet. Results show that the jet does not penetrate deeply into the tube. Instead, it moves downstream along a spiral created by the swirling flow in the absence of the jet. Consequently, the disturbances created by the jet are limited to a small region around the jet, and the reversed flow region along the tube core created by the swirling motion still remains intact. The turbulence field of the swirling flow is affected more by the jet than the mean flowfield. However, the disturbances created by the jet die off quickly. At two tube diameters away from the jet and farther downstream, the mean flow and turbulence fields exhibit behavior characteristic of the swirling flow alone. This demonstrates that the decay of the jet is fairly complete within this region. Finally, as the jet momentum is increased, the jet's effect is also noted in regions other than along the jet trajectory. This indicates jet-bifurcation behavior at high jet momentum.

I. Introduction

THE phenomenon of jets discharging normally or at an angle to a swirling or nonswirling crossflow is of practical interest to many areas of engineering. For example, in the environmental area, the phenomenon is found in the discharge of effluents into the atmosphere and moving streams of water. In gas turbine applications, the phenomenon is found commonly in the injection of secondary and dilution air jets into the combustor. The efficient dispersion of the effluents and the thorough mixing of the incoming air with the fuel and combustion products depend to a great extent on the resulting flowfield created by the jet. In order to optimize the various parameters that govern the performance of these systems, a thorough understanding of this type of flow is essential. As a result, numerous studies have been carried out on jets discharging into a crossflow.[1]

Most of the investigations in the past have concentrated on jets discharging normally into a uniform crossflow. Although the range of parameters investigated are large and include jet diameter, jet incident angle, jet-to-crossflow velocity and momentum flux ratios, and temperature and density differences between jet and crossflow fluid, little is known of the effects of swirl on such a phenomenon. Since fairly complete reviews of past work have been provided by Schetz[1] and Crabb et al.,[2] only a brief discussion of the more recent work will be outlined below.

In the area of jets discharging into uniform crossflows, the studies of Crabb et al.[2] and Atkinson et al.[3] should be mentioned. As for jets discharging into swirling crossflows, the most recent studies are provided by Ferrell et al.,[4,5] Ong et al.,[6] and Koutmos and McGuirk.[7,8]

Crabb et al.[2] used a laser Doppler anemometer (LDA) to examine the near field of a jet discharging into a uniform cross stream and hot wires to study the flow far downstream. Their results confirmed and quantified the double vortex characteristics of the jet flow and showed that the phenomenon was associated with fluid emanating from the jet. Also, the developing jet was characterized by strong anisotropy associated with the acceleration of the freestream around the jet and into its wake. Opposing jets discharging into a uniform crossflow were studied by Atkinson et al.[3] For velocity ratios greater than one, they found that the jets bifurcate about a vertical plane to form two symmetrical cores of mixed jet fluid. This bifurcation was not observed for velocity ratios equal to or less than one.

The characteristic flow patterns found in jets normal to uniform crossflows were not observed in jets discharging into swirling crossflows.[4-6] Here, for a given swirl number in the crossflow, the jet was observed to follow a spiral path, independent of the jet-to-crossflow velocity ratio. When the swirl number was increased, the spiral action of the jet was observed to be even more intense, and the jet tends to disperse more rapidly. The studies conducted by Ferrell et al.[4,5] concentrated on flow visualization only and no quantitative measurements were presented. Ong et al.[6] presented hot-wire measurements of the mean flowfield for two swirler vane angles of 45 and 70 deg. Their results confirmed the flow visualization observations of Ferrell et al.;[4,5] namely, that jet dispersion is highly dependent on swirl. However, in spite of the more detailed quantitative study, the effects of swirl on jet penetration were not quantified. As a result, the effects of swirl on jet penetration and the jet's effect on the swirling turbulence field are not known. On the other hand, Koutmos and McGuirk[7,8] used an LDA system to measure the flow characteristics. However, their interest was in multiple jet injections into swirling crossflows. Consequently, characteristics of single jets discharging into swirling crossflows are not known.

The present investigation makes a first attempt to measure single jet characteristics in the presence of a swirling crossflow. Ferrell et al.[4,5] and Ong et al.[6] have studied the same phenomenon visually and quantitatively using hot wires by varying the jet-to-crossflow velocity ratio from 2 to 6 and the vane angle in the swirler from 0 to 70 deg. These

Received Dec. 26, 1985; revision received June 18, 1986.

*Research Associate, Mechanical and Aerospace Engineering Department.

†Professor, Mechanical and Aerospace Engineering Department.

conditions give total jet to total axial flow momentum ratios of 0.04–0.36. In order to complement their studies, the present investigation is carried out at two higher total momentum ratios of 0.43 and 0.96 but at a fixed swirl number of $S=2.25$, which roughly corresponds to their 70-deg vane angle. Here, $S \simeq \tan\psi$ is assumed and ψ is the constant vane angle of the swirler. Therefore, the present study would provide some preliminary information on the effect of jet momentum on jet penetration in the presence of swirl.

II. Experimental Setup

The swirling flow facility of So et al.[9] is modified for the present experiments. In that facility, a vane swirler with a vane angle of 66 deg (which gives an overall swirl number S of 2.25) is mounted inside a Plexiglas tube with a diameter (D_T)of 125 mm. The swirler has a concentric jet with an 8.73-mm diam. For the present study, the concentric jet is blocked off and the vane swirler only produces a swirling flow in the tube. Instead, another jet nozzle is installed radially to the tube at one D_T downstream of the swirler. The jet nozzle is identical to the one in the vane swirler and is designed with a sudden expansion from 6.35 to 8.73 mm in diameter. Therefore, the jet nozzle exit diameter is $D_j=8.73$ mm. The design ensures turbulent jet flow even for low Reynolds numbers. This arrangement is essentially similar to the test facility of Ferrell et al.[4,5] and Ong et al.[6] The Plexiglas tubing forms part of the test section of an open-jet wind tunnel. Flow through the wind tunnel is provided by a blower that operates in the suction mode and is powered by a 25-hp variable-speed motor. Thus, average mean flow velocity up to 30 m/s in the test section can be obtained. For this investigation, air is used as the working fluid for both the jet and the swirling flow. Further details of the facility are given in Ref. 9, and a schematic of the test section setup is shown in Fig. 1.

A standard DISA model 55L LDA equipped with a DISA model 55N10 frequency shifter is used to measure the instantaneous axial velocity, $\tilde{u}$. The coherent light source is provided by a 15-mw helium-neon laser (wave length $\lambda=632.8$ nm) and the optics employed resulted in an ellipsoidal measuring volume of $\sim 1\times 0.1$ mm. Thus, the spatial resolution of the LDA technique used in the present setup is not better than 1/125. To improve the LDA signal quality and frequency resolution, artificial seeding provided by a DISA model 55L18 seeding generator is used. The generator generates liquid (50% water and 50% glycerin) droplets centered around 1 μm in size. The droplets are partly deposited through the seeding holes (shown in Fig. 1) and partly carried into the flow through the normal jet. Data handling and reduction procedures established in Ref. 9 are used again in the present investigation.

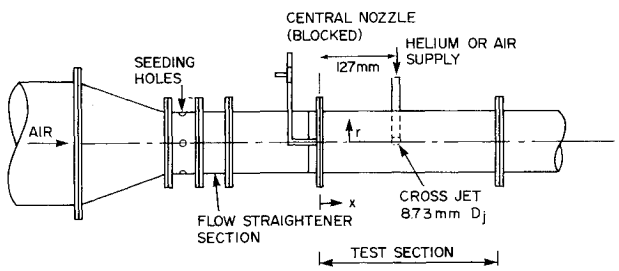

Fig. 1 Details of test section.

Altogether, two experiments are carried out. The jet velocity is fixed at $U_j=66.8$ m/s for both experiments, whereas the average mean axial velocities of the flow upstream of the vane swirler (U_{av}) are set at 7.11 m/s and 4.76 m/s, respectively. Therefore, this gives two velocity ratios, U_j/U_{av}, of 9.40 and 14.03; two momentum flux ratios, $J=U_j^2/U_{av}^2$, of 88.3 and 196.9; and two total momentum ratios, $M_j/M=D_j^2U_j^2/D_T^2U_{av}^2$, of 0.43 and 0.96. The jet Reynolds number, $Re_j=U_jD_j/\nu$, is $\sim 3.8\times 10^4$. In addition to the jet flowfield, the swirling flowfield in the absence of the normal jet also is measured so that the effect of the jet on the swirling flow can be identified and analyzed.

III. Measurement Procedure

The LDA system used by So et al.[9] is equipped with a two-dimensional traversing mechanism. Therefore, the sampling volume can be moved parallel or perpendicular to the centerplane of the test section. This limited access would not yield enough measurements to define the flowfield created by a deflected jet moving along a spiral path, as noted in Refs. 4-6. Ong et al.[6] used a six-orientation hot-wire probe to measure the three-dimensional flowfield downstream of the injection jet. Their measurements were obtained along six different angular positions at any one stream location. The results were reported in the form of r-x plots to aid visualization of the three-dimensional flowfield. The authors concluded from their measurements that the maximum errors for the Reynolds stresses were 25 to $\sim 100\%$ in certain regions of the flow. Consequently, they did not report the turbulence measurements in their paper. Furthermore, due to the manner in which the mean flow velocities were presented, jet penetration was difficult to assess. An alternative way of determining jet mixing behavior and penetration is to measure the jet growth along the spiral path. In order to follow this spiral path, either the tube is rotated so that the jet path is moved to the horizontal centerplane for measurement or the light beams are steered to follow the jet path. The former option requires knowing the spiral path a priori; the latter alternative requires an elaborate traversing mechanism. Since it is much less costly and more convenient to rotate the tube, it was decided to use flow visualization to define the jet path before actual measurements were carried out.

Simple flow visualization technique is used to define the jet path. The jet flow is uniformly seeded with liquid droplets centered around 1 μm in size. A laser beam and a glass rod are used to create a sheet of light to illuminate the droplets in the tube. This way the jet path is clearly visible. The flow visualization experiment is carried out for several M_j/M values ranging from 0.07 to ~ 1. Results show that the jet follows the spiral path shown in Fig. 2. For ease of reference later on, the side where the jet enters the tube is designated the jet side and the opposite side where the laser beams enter is called the laser side (Fig. 2). The jet transfers

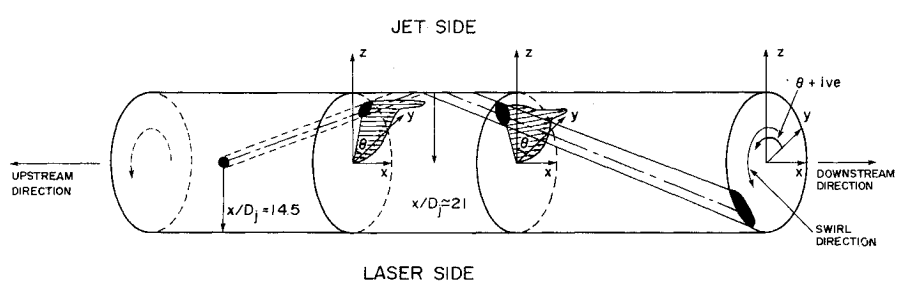

Fig. 2 Schematic representation of spiral path of jet discharging normally into a swirling crossflow.

from the jet side to the laser side and back to the jet side as it moves downstream. The spiral path is essentially determined by the motion of the swirling flow and does not differ much for the range of M_j/M investigated. On the other hand, the spiral path slowly decays in the stream direction. Consequently, the jet trajectory shown in Fig. 2 is not a perfect spiral. No effort has been made to photograph the flowfield. Instead, the jet trajectory is traced out and a schematic representation is shown in Fig. 2. Once the jet path is known, the velocity field measurements can be carried out in the following manner.

Initially, the jet nozzle is positioned in the horizontal centerplane. This location is designated by $\theta = 0$ deg and $x/D_j = 14.5$, where x is measured from the exit plane of the swirler. Therefore, once the jet path is known from flow visualization, the θ angle through which the tube has to be rotated at any axial location to position the jet path in the horizontal centerplane for measurement can be determined. The angle θ is uniquely related to x/D_j and could be measured with an accuracy of ± 1 deg. When this is accomplished, the tube is further rotated slightly around this θ position to give a maximum radial extent of jet width for measurement. If necessary, measurements are also carried out across different angular planes positioned at a fixed x/D_j location so that a better definition of the jet flowfield can be constructed. Several axial positions that range from $x/D_j = 16$ to 40 are selected for detailed profile measurements. Since the jet nozzle is located at $x/D_j = 14.5$, the above axial locations correspond to 1.5-25.5 jet diameter downstream of the jet nozzle. The swirling flow in the absence of the normal jet is axisymmetric. Therefore, only measurements across the horizontal centerplane given by $\theta = 0$ deg for all x/D_j locations traversed are made, and these are used to compare with the measurements obtained with the normal jet present.

IV. Presentation of Results

In order to elucidate the characteristics of jets normal to swirling crossflows, the results are organized into the following three sections for presentation and discussion. These are: 1) mean axial velocity profiles, 2) turbulence distribution, and 3) jet penetration.

Mean Axial Velocity Profiles

Profile measurements of the mean axial velocity $U(r)$ at seven different x locations are plotted in Figs. 3 and 4 for the cases of $M_j/M = 0.43$ and 0.96, respectively. Also shown in these figures are the corresponding swirling flow data in the absence of the normal jet. The velocity is normalized with respect to U_{av}, and the radial coordinate r is normalized with respect to $R = D_j/2$. For the $M_j/M = 0$ case, the data are obtained from measurements carried out at $\theta = 0$ deg for all x/D_j locations traversed. As for the $M_j/M = 0.43$ and 0.96 cases, the data are from measurements taken at $x/D_j = 16$, 18, 20, 24, 28, 32, and 40, corresponding to different θ's. Since x/D_j are uniquely related to θ, the jet trajectory traced out in the flow visualization experiment gives the corresponding θ values as -12, -31, -68, $+40$, -18, -90, and -12, respectively. Here, the sign convention shown in Fig. 2 for θ is adopted.

The first three locations ($x/D_j = 16$, 18, and 20) show large differences in the U profiles between the background swirling flow and a normal jet discharging into a swirling flow. However, the disturbances created by the jet are noted only in the jet side (Figs. 3 and 4) and not in the laser side (opposite to where the jet is being introduced into the tube). This is in agreement with the flow visualization results (Fig. 2), which show that the jet does not penetrate deeply into the swirling flow and the jet fluid moves along a spiral path. The jet's presence, which is observed to be in the jet side at $14.5 \le x/D_j < 20$, transferred to the laser side at $20 < x/D_j < 32$. This is again consistent with the observed spiral motion of the jet. When the jet momentum is increased to $M_j/M = 0.96$, the jet penetration increases slightly and the jet's effect can be felt in other regions of the tube in the downstream direction.

In order to map out the behavior of the flowfield for this case ($M_j/M = 0.96$) in more detail, measurements across five different angular planes aside from the horizontal centerplane are carried out at several x/D_j locations. These results could be presented in profile plots similar to Figs. 3 and 4. However, a much clearer presentation of the jet's effect can be made by showing the contours of the axial velocity component at different x/D_j locations. Since the number of planes where measurements are available are limited, the velocity contours are approximate. As a result, only a limited number of equivelocity contours at $x/D_j = 18$ and 28 are shown in Figs. 5 and 6, respectively, which illustrate the swirling flow patterns as influenced by a normal jet. In the absence of the jet, the contour should be a complete ring for a confined swirling flow. At $x/D_j = 18$, the plot gives a horseshoe appearance for the $U/U_{av} = 1.5$ contour, indicating the limited influence of the jet on the swirling flow (Fig. 5). The largest effect of the jet, however, still centers around the jet in the jet side only and is clearly shown by the location of the velocity maximum ($U/U_{av} = 1.6$). This is true for the two M_j/M cases investigated. As the jet moves downstream, its effect on the

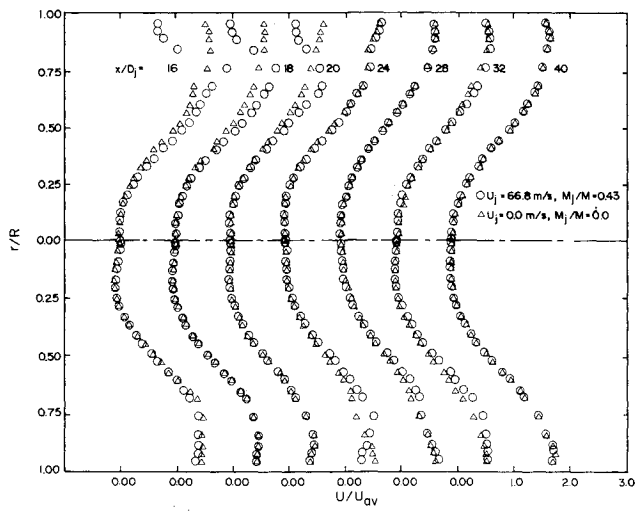

Fig. 3 Comparison of $U(r)$ profiles measured along the jet for the case of $M_j/M = 0.43$ with $M_j/M = 0$.

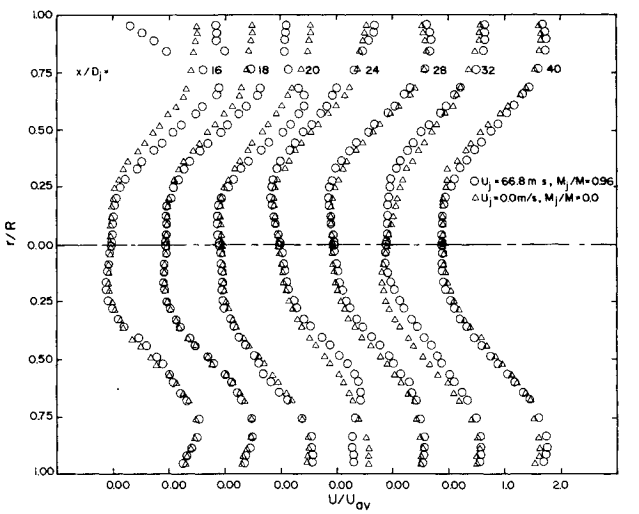

Fig. 4 Comparison of $U(r)$ profiles measured along the jet for the case of $M_j/M = 0.96$ with $M_j/M = 0$.

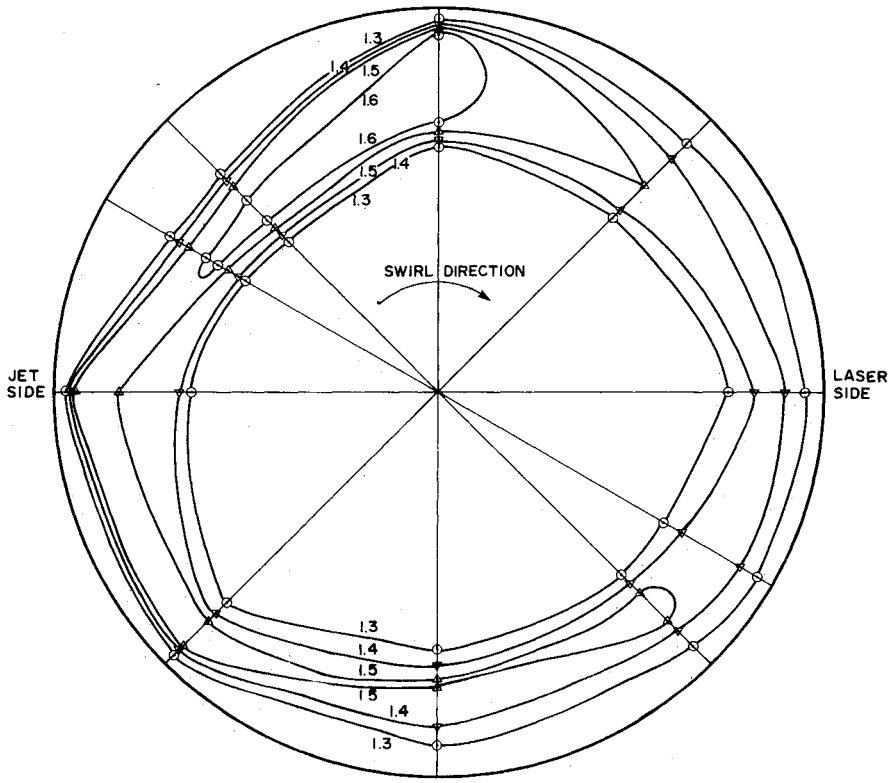

Fig. 5 Contour plots of the velocity U/U_{av} at $x/D_j = 18$ for the case of $M_j/M = 0.96$.

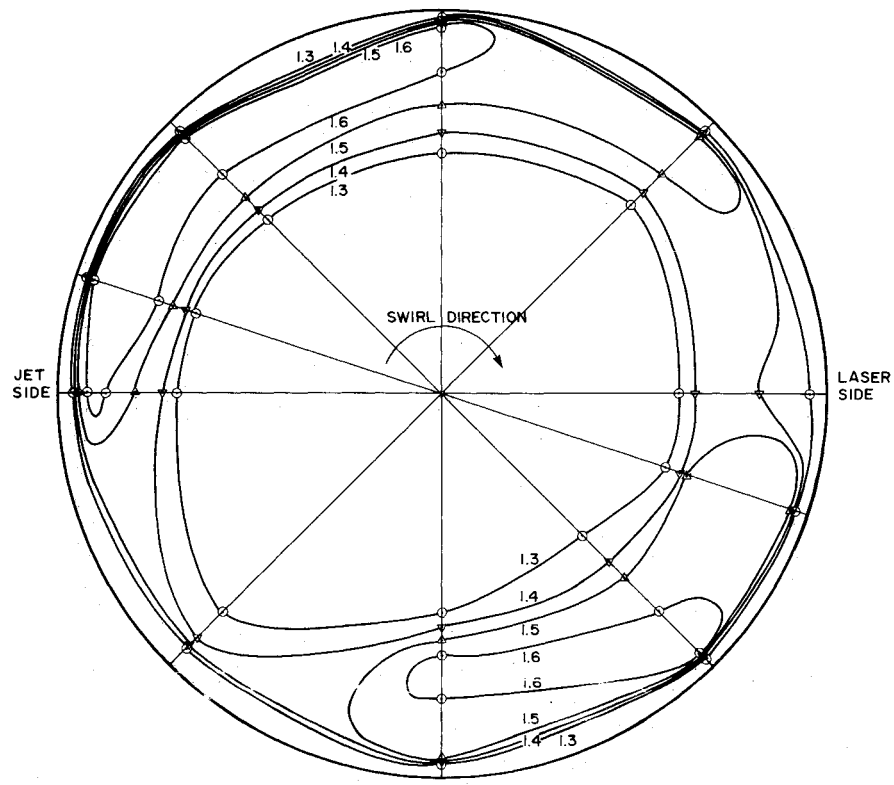

Fig. 6 Contour plots of the velocity U/U_{av} at $x/D_j = 28$ for the case of $M_j/M = 0.96$.

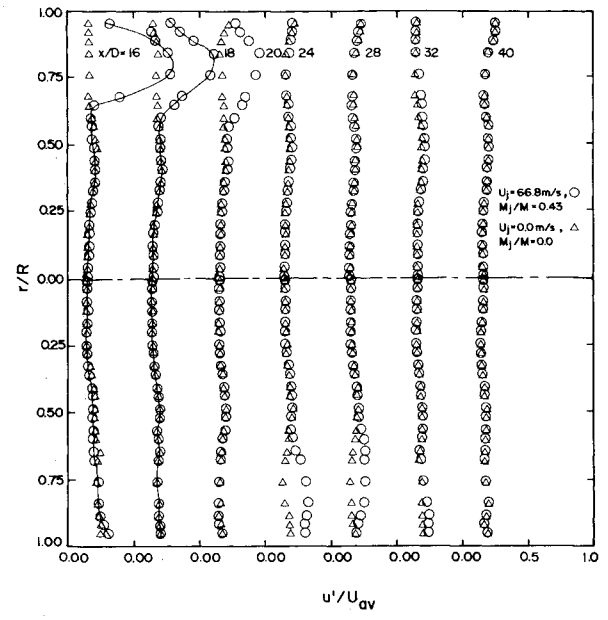

Fig. 7 Comparison of u' profiles measured along the jet for the case of $M_j/M=0.43$ with $M_j/M=0$.

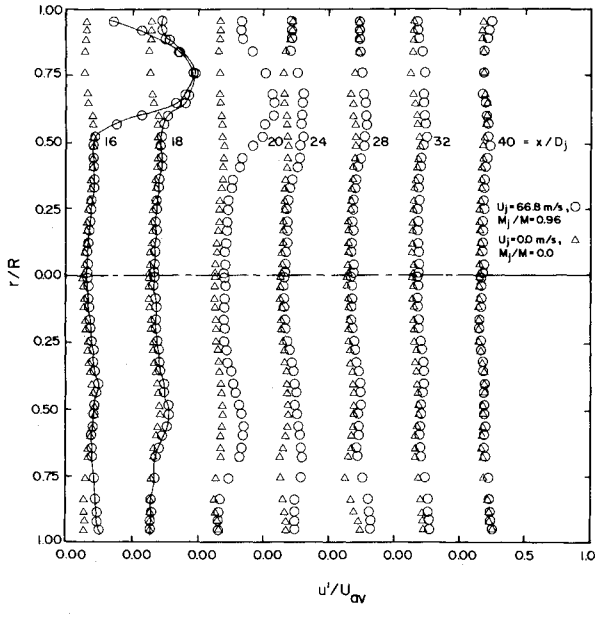

Fig. 8 Comparison of u' profiles measured along the jet for the case of $M_j/M=0.96$ with $M_j/M=0$.

swirling flow differs depending on the jet momentum, M_j. For the $M_j/M=0.43$ case, the jet's effect is still confined to the region along the spiral path (Fig. 3). However, this is not the case for the large momentum jet ($M_j/M=0.96$). At $x/D_j=28$, another region of local velocity maximum ($U/U_{av}=1.6$) is observed on the laser side (compare Figs. 5 and 6), clearly indicating that the jet has bifurcated to the opposite side. Simultaneously, the horseshoe shape of the $U/U_{av}=1.5$ contour breaks up into two regions. The measurements also show that the presence of the jet is no longer noticeable at $x/D_j=32$ for the $M_j/M=0.43$ case (Fig. 3), but it is still measurable at $x/D_j=40$ for the $M_j/M=0.96$ case (Fig. 4). These characteristics differentiate the behavior of the low- and high-momentum jets in a swirling crossflow.

The characteristics of jets discharging normally into swirling crossflows do show some similarities with jets discharging into a uniform crossflow. For example, the jet bends in the direction of the crossflow and the back of the jet has a decreased velocity while the front is forced to accelerate (Figs. 3 and 4). Further evidence that the jet does not penetrate deeply into the main flow is provided by the fact that the reversed flow due to swirl along the tube centerline is still prevalent (Figs. 3 and 4). Also, no reversed flow is noticed behind the jet, as is commonly observed when the crossflow is a uniform stream.[2]

Turbulence Distributions

The rms turbulent normal stress profiles (u'/U_{av}) obtained at the various x/D_j locations are presented in Figs. 7 and 8. These plots show the evolution of the turbulence flowfield in the flow direction for the two jets studied. The contours of u'/U_{av} at $x/D_j=18$ and 28, constructed in a manner similar to those shown in Figs. 5 and 6, are given in Figs. 9 and 10. In addition, the turbulence characteristics of the swirling flow alone are shown in Figs. 7 and 8 for comparison. Therefore, any variation from this background turbulence field is an indication of the jet's influence.

The jet's effects observed in Figs. 7 and 8 are essentially similar to those noted in Figs. 3 and 4, except that they are a lot more pronounced. This shows that the jet, upon entering the swirling crossflow, undergoes a process that rapidly transfers its mean kinetic energy into turbulence energy. As a result, the rms turbulent normal stress u' is several times greater than the swirling flow u' within the jet mixing region (Figs. 7 and 8). For the case $M_j/M=0.96$, the jet's influence in other regions away from the jet is clearly shown in the contour plots of Figs. 9 and 10. For example, Fig. 9 shows the large effect of the jet in an angular sector that occupies more than one quarter of the whole tube. The jet's effect on the horizontal centerplane near the laser side of the tube is also shown. Again, the ring contour of the swirling flow is not observed, except in the pipe core where the jet's presence is not felt (Fig. 9). From the mean flow results, jet bifurcation effects are noticeable when $x/D_j=28$. However, they are quite distinct in the u' measurements, even at $x/D_j=18$. This shows that the rapid transfer of the jet's mean kinetic energy into turbulence energy is being felt all over the turbulence field before the jet's effect is felt on the mean flowfield. The reason for this is the faster turbulent time scales compared to the mean convective time scales. As the jet moves downstream, the u'/U_{av} contours show the gradual approach of the turbulence field toward that characteristic of the swirling flow alone. As in the mean field result, this behavior is only peculiar to the large momentum jet case ($M_j/M=0.96$). For the $M_j/M=0.43$ case, the jet's effect on the turbulence field is limited to a small region around the jet and along the spiral path. As before, the jet's presence is observed to disappear at $x/D_j=32$ (Fig. 7), while for the $M_j/M=0.96$ case, the jet's effect is still quite pronounced at $x/D_j=32$ (Fig. 8).

The results presented thus far show that the jet moves along a spiral path determined by the motion of the swirling crossflow. When the jet momentum is small, the jet's influence is essentially confined within this spiral path. As the jet momentum is increased to $M_j/M\sim 1$, the jet's influence is observed to spread across the flow, and the mean and turbulence field measurements indicate jet bifurcation at some distance downstream of the jet nozzle. The experiment of Ong et al.[6] was carried out at $M_j/M=0.16$. Consequently, jet bifurcation behavior was not observed. The present experiment seems to indicate that jet bifurcation behavior would only appear for $M_j/M>0.5$.

Jet Penetration

In spite of the fact that the present measurements do not span a wide range for M_j/M and S, an attempt will be made to assess the effect of swirl on jet penetration. For isothermal, homogeneous jet mixing, jet penetration is defined usually in terms of the jet centerline trajectory. Normally,

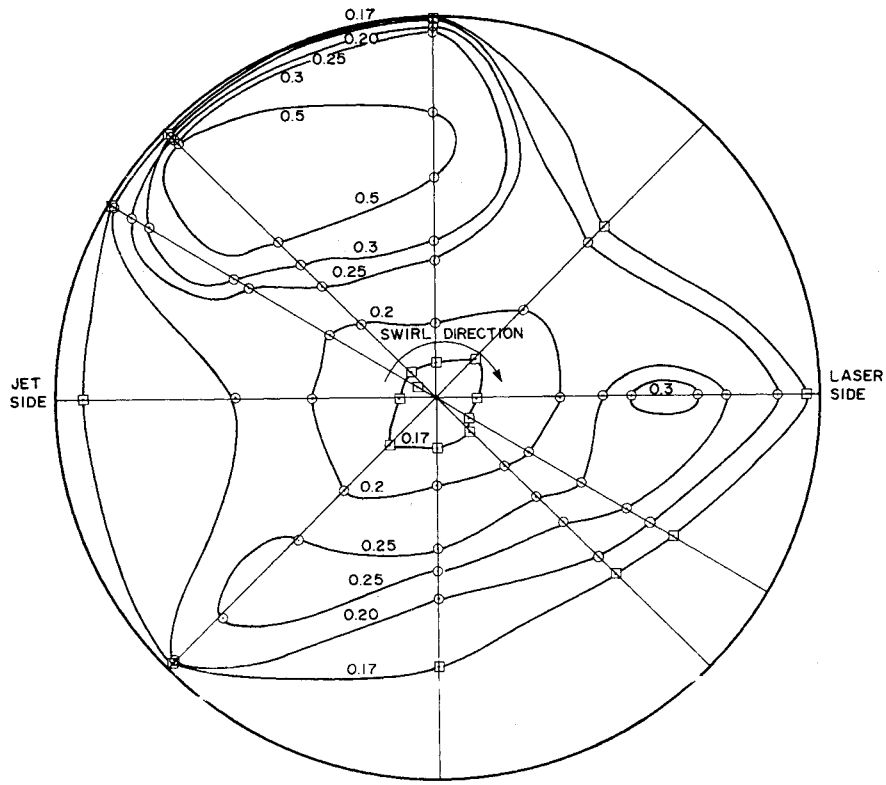

Fig. 9 Contour plots of u'/U_{av} at $x/D_j = 18$ for the case of $M_j/M = 0.96$.

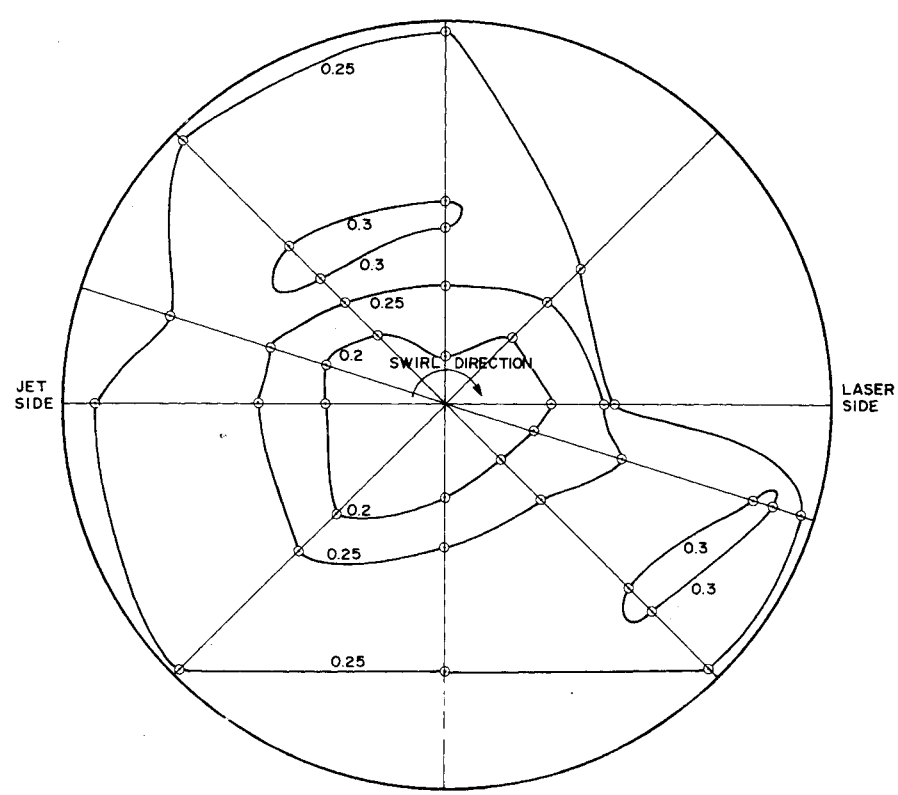

Fig. 10 Contour plots of u'/U_{av} at $x/D_j = 28$ for the case of $M_j/M = 0.96$.

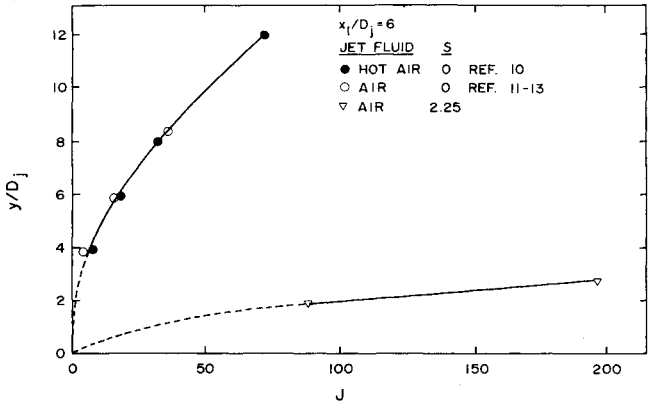

Fig. 11 Effects of swirl on jet penetration.

the mean axial velocity U is used to define the jet path, which is taken to be the locus of maximum U. When heated jets are considered, the jet path can also be defined as the locus of the maximum mean temperature. For the present, the locus of the maximum U is used to define the jet path and hence the jet penetration.

The effect of swirl on jet penetration is examined by comparing the present results with those of Kamotani and Greber,[10] Ramsey and Goldstein,[11] Keffer and Baines,[12] and Jordinson[13] on jets discharging normally into a uniform crossflow. Since their results are presented in terms of J, the momentum flux ratio, rather than M_j/M, the comparison is made with jet penetration at a fixed distance downstream of th jet entrance plotted vs J. The data at $x_1/D_j = 6$ (where x_1 measures from the jet nozzle centerplane) are chosen and the plot is given in Fig. 11. It can be seen that swirl decreases jet penetration and hence prevents jet mixing with the crossflow. The effect is quite dramatic. Even though not enough data are available to define the curve with swirl ($S = 2.25$) properly, the effect of swirl on jet penetration is clearly indicated by the present results.

V. Conclusions

Jets discharging normally into a swirling crossflow have been studied experimentally. The jet exit velocity and the swirl number of the crossflow are constant throughout this investigation, whereas the average mean axial velocity is varied. Two cases are examined. One has J and M_j/M equal to 88.3 and 0.43, respectively; the other has corresponding values of 196.9 and 0.96. Results show that the jet fluid follows a spiral path as it moves downstream. The spiral path is essentially determined by the swirling motion of the crossflow. Upon entering the swirling crossflow, a substantial amount of the jet mean kinetic energy is converted into turbulence energy, thus giving rise to a very high level of turbulence in the jet mixing region. For the $M_j/M = 0.43$ case, the jet's influence is only felt in a region around the jet path. However, the jet's influence is felt in other regions of the tube when M_j/M is increased to 0.96. The measurements also indicate jet bifurcation for this case at $x/D_j = 28$; however jet bifurcation is not observed for the $M_j/M = 0.43$ case. Finally, swirl is found to have a dramatic effect on jet penetration. At a swirl number of 2.25, jet penetration is found to decrease by a factor of ~ 5 at six jet diameters downstream of the jet.

Acknowledgment

This research is supported by Naval Weapons Center, China Lake, CA, under Contract N60530-85-C-0191.

References

[1]Schetz, J. A., *AIAA Progress in Astronautics and Aeronautics: Injection and Mixing in Turbulent Flow*, Vol. 68, AIAA, New York, 1980.

[2]Crabb, D., Durao, D.F.G., and Whitelaw, J. H., "A Round Jet Normal to a Crossflow," *Journal of Fluids Engineering*, Vol. 103, 1981, pp. 142-153.

[3]Atkinson, K. N., Khan, Z. A., and Whitelaw, J. H., "Experimental Investigation of Opposed Jets Discharging Normally into a Cross-stream," *Journal of Fluid Mechanics*, Vol. 115, 1982, pp. 493-504.

[4]Ferrell, G. B., Abujelala, M. T., Busnaina, A. A., and Lilley, D. G., "Lateral Jet Injection into Typical Combustion Flowfields," AIAA Paper 84-0374, 1984.

[5]Ferrell, G. B., Aoki, K., and Lilley, D. G., "Flow Visualization of Lateral Jet Injection into Swirling Crossflow," AIAA Paper 85-0059, 1985.

[6]Ong, L. H., McMurry, C. B., and Lilley, D. G., "Hot-Wire Measurements of a Single Lateral Jet Injected into Swirling Crossflow," AIAA Paper 86-0055, 1986.

[7]Koutmos, P. and McGuirk, J. J., "Isothermal Measurements of the Internal Flowfield in a Water Model Can-Type Gas Turbine Combustor," Rept. F8/84/14, Imperial College, Mechanical Engineering Dept., 1984.

[8]Koutmos, P. and McGuirk, J. J., "Investigation of Swirler/Dilution Jet Flow Split on Primary Zone Flow Patterns in a Water Model Can-Type Combustor," ASME Paper 85-GT-180, 1985.

[9]So, R.M.C., Ahmed, S. A., and Mongia, H. C., "Jet Characteristics in Confined Swirling Flow," *Experiments in Fluids*, Vol. 3, 1985, pp. 221-230.

[10]Kamotani, Y. and Greber, I., "Experiments on a Turbulent Jet in a Cross Flow," *AIAA Journal*, Vol. 10, Nov. 1972, pp. 1425-1429.

[11]Ramsey, J. W. and Goldstein, R. J., "Interaction of a Heated Jet with Deflecting Stream," NASA CR-72613, 1970.

[12]Keffer, J. F. and Baines, W. D., "The Round Turbulent Jet in a Cross Wind," *Journal of Applied Mechanics*, Vol. 15, 1963, pp. 481-490.

[13]Jordinson, R., "Flow in a Jet Directed Normal to the Wind," Aeronautical Research Council, R&M No. 30.4, 1958.